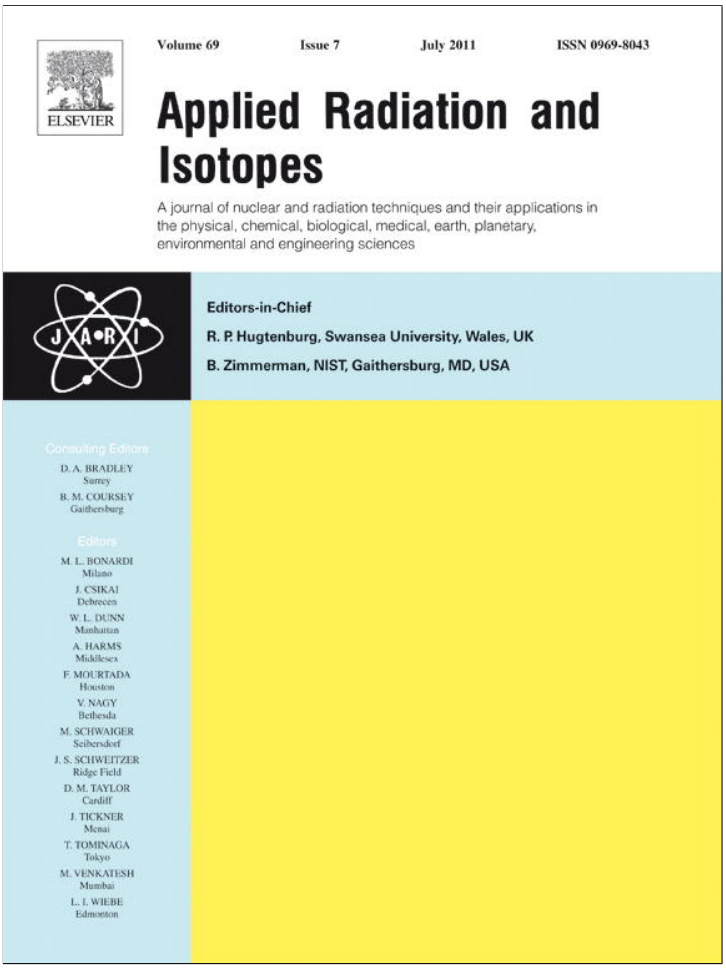

Applied Radiation and Isotopes 69 (2011) 960–964

Contents lists available at ScienceDirect

Applied Radiation and Isotopes

journal homepage: www.elsevier.com/locate/apradiso

Measurements of k_0 and Q_0 values for $^{64}Zn(n,\gamma)^{65}Zn$ and $^{68}Zn(n,\gamma)^{69m}Zn$ reactions with covariance analysis

M.S. Dias *, V. Cardoso, M.F. Koskinas, I.M. Yamazaki, R. Semmler, M. Moralles, G.S. Zahn, F.A. Genezini, M.O. de Menezes, A.M.G. Figueiredo

Instituto de Pesquisas Energéticas e Nucleares (IPEN-CNEN/SP), Centro do Reator de Pesquisas – CRPq, C.P. 11049, Pinheiros, 05422-970 – São Paulo – SP, Brazil

ARTICLE INFO

Article history:
Received 3 January 2011
Received in revised form
16 March 2011
Accepted 17 March 2011
Available online 7 April 2011

Keywords:
k_0 Method
Gamma-ray spectrometry
Zn isotopes
Activation analysis
Nuclear reactor

ABSTRACT

The values of k_0 and Q_0 for $^{64}Zn(n,\gamma)^{65}Zn$ and $^{68}Zn(n,\gamma)^{69m}Zn$ reactions were determined experimentally. The irradiations were performed near the core of the IEA-R1 3.5 MW nuclear research reactor of the Nuclear and Energy Research Institute – IPEN-CNEN/SP, in São Paulo, Brazil. The results for the neutron field parameters f and α were 49.7(19) and $-1.1(31)\times10^{-3}$, respectively. The resulting values of k_0 and Q_0 for $^{64}Zn(n,\gamma)^{65}Zn$ reaction were $5.63(8)\times10^{-3}$ and 1.69(6), respectively, and the corresponding values for $^{68}Zn(n,\gamma)^{69m}Zn$ reaction were $4.00(6)\times10^{-4}$ and 2.34(4), respectively. These results were compared with the literature.

1. Introduction

The use of the k_0 method for quantitative reactor Neutron Activation Analysis (NAA) is a well-known technique for determining multi-element concentrations in different materials. In order to achieve good results, there is a continuing need to improve the accuracy of k_0 parameter for several neutron capture reactions, as pointed out by Firestone (2008). Among these reactions, $^{64}Zn(n,\gamma)^{65}Zn$ can be considered particularly important because it can be used for a twofold purpose: as neutron flux monitor and for Zn concentration measurements. Recently, an inconsistency was observed between the k_0 values from the Atomic and Nuclear Data Tables (De Corte and Simonits, 2003) and from the Atlas of Neutron Resonances (Mughabghab, 2006). This fact motivated the present work, which is focused on the measurement of k_0 and Q_0 values for $^{64}Zn(n,\gamma)^{65}Zn$ reaction. As a complementary work and consistency test, the k_0 and Q_0 values for $^{68}Zn(n,\gamma)^{69m}Zn$ reaction were also measured. The irradiations were performed near the core of the IEA-R1 3.5 MW swimming-pool nuclear research reactor of the Instituto de Pesquisas Energéticas e Nucleares (Ipen-Cnen/SP – Nuclear and Energy Research Institute), in São Paulo, Brazil.

2. Materials and methods

2.1. k_0 equations

In the epithermal region the neutron spectrum follows approximately $1/E^{1+\alpha}$. For the present work the parameter α was obtained by the Cd-ratio multi-monitor method, described by De Corte (1987), measuring the slope of the curve $Y_i = a + \alpha X_i$, where:

$$X_i = \ln \bar{E}_{r,i}$$

and

$$Y_i = \ln\left[\frac{(\bar{E}_{r,i})^{-\alpha} G_{th,i}}{(F_{Cd,i}R_{Cd,i}-1)Q_{0,i}(\alpha)G_{e,i}}\right] \quad (1)$$

index i refers to the ith target nucleus, $\bar{E}_{r,i}$ is the effective resonance energy, $F_{Cd,i}$ is the Cd transmission factor for epithermal neutrons, $R_{Cd,i}$ is the cadmium ratio; $Q_{0,i}(\alpha)$ is the ratio between the resonance integral and the thermal cross section as a function of α and $G_{th,i}$ and $G_{e,i}$ are the self-shielding correction factors for thermal and epithermal neutrons, respectively.

The ratio f between thermal and epithermal fluxes was taken from the inverse of the intercept of this curve and is given by:

$$f = (F_{Cd,i}R_{Cd,i}-1)Q_{0,i}(\alpha)G_{e,i}/G_{th,i} \quad (2)$$

since the Y_i values depend on the α parameter, an iterative procedure was performed until convergence was achieved.

* Corresponding author. Tel.: +55 11 3133 8779; fax: +55 11 3133 9960.
E-mail address: msdias@ipen.br (M.S. Dias).

0969-8043/$ - see front matter © 2011 Elsevier Ltd. All rights reserved.
doi:10.1016/j.apradiso.2011.03.026

The Q_0 value was calculated from $Q_0(\alpha)$, which is given by the following expression taken from De Corte (1987):

$$Q_{0,i}(\alpha) = \frac{F_{Cd,c}R_{Cd,c}-1}{F_{Cd,i}R_{Cd,i}-1} \times \frac{G_{th,i}}{G_{th,c}} \times \frac{G_{e,c}}{G_{e,i}} Q_{0,c}(\alpha) \quad (3)$$

the index c corresponds to the comparator (Au). The relationship between $Q_0(\alpha)$ and Q_0 is given by De Corte (1987):

$$Q_{0,i}(\alpha) = \frac{Q_{0,i}-0.429}{(\bar{E}_{r,i})^{\alpha}} + \frac{0.429}{(2\alpha+1)(0.55)^{\alpha}} \quad (4)$$

From this expression, it can be noted that $Q_0(\alpha)=Q_0$ when α is equal to zero. For the comparator (Au), $Q_{0,c}(\alpha)$ was obtained from the published value of $Q_{0,c}$ (De Corte and Simonits, 2003) inserted into Eq. (4) and the result was applied to Eq. (3). For the target sample the $Q_{0,i}(\alpha)$ value was obtained first and then applied to Eq. (4), in order to obtain $Q_{0,i}$.

The parameter k_0 was obtained by the following relationship (De Corte, 1987):

$$k_{0,i} = \frac{A_{sp,i}-((A_{sp,i})_{Cd}/F_{Cd,i})}{A_{sp,c}-((A_{sp,c})_{Cd}/F_{Cd,c})} \times \frac{G_{th,c}}{G_{th,i}} \times \frac{\varepsilon_c}{\varepsilon_i} \quad (5)$$

where $k_{0,i}$ is the k_0 factor with respect to the comparator (Au); $(A_{sp,i})_{Cd}$ and $A_{sp,i}$ are the total absorption gamma-ray peak area of the reaction products, obtained by HPGe gamma-ray spectrometry measurements, with and without cadmium cover, respectively. These values were corrected for saturation, decay time, cascade summing, geometry, measuring time and mass; ε_c and ε_i are the peak efficiencies for the comparator and target nuclei, respectively.

The values of effective resonance energy $\bar{E}_{r,i}$ and Q_0 to be applied in Eqs. (1)–(4) were taken from Kolotov and De Corte (2002). The values of G_{th} and G_e were calculated on basis of expressions given by Martinho et al. (2003) and Martinho et al. (2004), respectively, using gamma-ray width (Γ_γ) and neutron width (Γ_n) taken from ENDF/B-VII (2010). For the cases where the target has several proeminent resonances (^{64}Zn, ^{94}Zr and ^{96}Zr) an average value was calculated. The resulting values of G_{th} and G_e are shown in Table 1.

The cadmium factors (F_{Cd}) were calculated by the average transmission in the Cd cover, applying cross section data from ENDF/B-VII (2010) and considering variation in the Cd thickness due to isotropic neutron flux. The following equation taken from Kodeli and Trkov (2007), was applied:

$$F_{Cd} = \frac{\int_0^{\infty} t(E)\sigma(E)\phi(E)\,dE}{\int_{E_{Cd}}^{E_3} \sigma(E)\phi(E)\,dE} \quad (6)$$

In the present work this equation has been approximated by:

$$F_{Cd} = \frac{\sum_i t(E_i)\sigma(E_i)\phi(E_i)\Delta E_i}{\sum_i \sigma(E_i)\phi(E_i)\Delta E_i} \quad (7)$$

where $t(Ei)$ is the transmission factor given by:

$$t(E_i) = e^{-N_{Cd}d\sigma_{Cd}(E_i)} \quad (8)$$

in this equation, N_{Cd} is the number density of cadmium atoms, d is the crossing distance inside the Cd layer and $\sigma_{Cd}(E)$ and $\sigma(E)$ are the Cd and sample absorption cross sections, respectively, taken from ENDF/B-VII (2010). The neutron spectrum $\phi(E_i)$ was assumed to follow the $1/E$ law. E_{Cd} and E_3 are the Cd cutoff energy and the upper energy limit, assumed to be 0.55 eV and 2 MeV, respectively.

ΔE_i corresponds to the ith energy bin from the Cd cross section library. The sample cross section value was interpolated to match the same energy found in the Cd cross section table.

In order to account for isotropic neutron incidence, the cadmium factors given by Eq. (7) have been averaged with respect to the solid angle Ω_i covered by the cadmium box, according to the following expression:

$$\bar{F}_{Cd} = \frac{\sum_k F_{Cd,\Omega_k}\Delta\Omega_k}{\sum_k \Delta\Omega_k} \quad (9)$$

The limits of upper integral in Eq. (6) are zero and infinity, opening the possibility for $\bar{F}_{Cd}$ to be larger than one. This can be explained considering that neutrons below the Cd cutoff energy may also contribute to sample activation. These two limits were considered in the calculation as equal to 1×10^{-5} eV and 2 MeV, respectively. The values obtained for $\bar{F}_{Cd}$ are shown in Table 2.

2.2. Sample preparation and irradiation

Samples of Au (0.10% and 0.13% Al alloys), Co (0.475% Al alloy), Zr, Zn and La (0.665% Al alloy) as well as pure Zr were used as flux monitors for determining α and f parameters at an irradiation position near the IEA-R1 reactor core. The selected samples for k_0 and Q_0 measurements were pure Zn foils 0.09 cm thick. The sample masses ranged from 5 mg (Zr) to 250 mg (Zn) and were measured within $\pm$20 μg uncertainty. The samples were wrapped with thin aluminum foils and positioned in the middle of an aluminum rabbit 7.0 cm long, 2.1 cm in diameter and 0.05 cm thick.

Two sets of samples were prepared: one with cadmium cover and the other without it. These two sets were irradiated during 60 min each, in sequence: the first with cadmium cover and the second without it. The minimum decay time before measurements was around 29 h.

The sample irradiation and measurement procedures were performed twice.

2.3. Efficiency calibration

Standard sources of ^{60}Co, ^{133}Ba, ^{152}Eu, and ^{166m}Ho, calibrated in a $4\pi\beta-\gamma$ coincidence system, were used for obtaining the HPGe gamma-ray peak efficiency as a function of the energy. These sources were prepared by dropping known aliquots of standard radioactive solutions on thin Collodion films 30 μg cm^{-2} thick with negligible gamma-ray attenuation. These

Table 1
Values obtained for G_{th} and G_e; the numbers inside parentheses are the uncertainties in the last digits (one standard deviation).

Target	G_{th}	G_e
^{197}Au	**1.0000(0)**	**0.9808(39)**
^{64}Zn	**0.9924(15)**	**0.9605(87)**
^{68}Zn	**0.9993(1)**	**0.9564(91)**
^{139}La	**0.9999(1)**	**0.9981(4)**
^{94}Zr	**0.9999(1)**	**0.9990(4)**
^{96}Zr	**1.0000(0)**	**0.9988(10)**
^{59}Co	**1.0000(0)**	**0.9971(6)**

Table 2
Values obtained for the cadmium transmission factor; the numbers inside parentheses correspond to uncertainties in the last digits (one standard deviation).

Target	$\bar{F}_{Cd}$
^{197}Au	0.9999 (4)
^{64}Zn	0.9928(19)
^{68}Zn	0.9985(12)
^{139}La	1.0160 (24)
^{94}Zr	0.9968(7)
^{96}Zr	0.9995(1)
^{59}Co	0.9909(20)

sources were positioned 17.9 cm away from the crystal front face. The peak area was calculated applying a sigmoidal background function as described by Dias et al. (2004). An accurate pulser was introduced in the gamma-ray spectrum close to the right edge, in order to perform dead time and pile-up corrections. A third degree polynomial in log–log scale was fitted between the HPGe peak efficiency and the gamma-ray energy, covering the 244–1408 keV energy range. The reduced chi-square resulted 1.48. The uncertainty in the interpolated efficiency was in the 0.47–0.69% range.

A second efficiency calibration was performed using ^{60}Co, ^{133}Ba, ^{137}Cs, ^{152}Eu and ^{241}Am standard sources supplied by the IAEA. These sources were sealed inside a 0.04 cm polyethylene plus 0.05 cm aluminum capsule and positioned at the same distance to HPGe crystal as the previous case. The peak area was calculated by means of a Genie 2000 software. The fitting was performed with a set of exponential functions combined with Monte Carlo calculations and covering the 53–1408 keV gamma-ray energy range. This function is given by Zevallos-Chávez et al. (2005):

$$\varepsilon(E_\gamma) = \left(P_1\, e^{-P_2.E_\gamma} + P_3\, e^{-P_4.E_\gamma}\right) e^{-P_5(0.05757E_\gamma^{-0.416} + 0.000465E_\gamma^{-2.943})} \quad (10)$$

where P_i are the fitting parameters. The constants appearing in the exponents come from Monte Carlo calculations and are the same for different crystal sizes, as described by Zevallos-Chávez et al. (2005). The reduced chi-square resulted 0.80. The uncertainty in the interpolated efficiency was in the 0.41–1.86% range. This latter large value was obtained at 53 keV of ^{133}Ba, which was the lowest fitted gamma-ray energy.

2.4. Covariance matrix methodology

The covariance matrix methodology is necessary for rigorous statistical analysis and was applied to all uncertainties involved. From the series expansion of a multi-parametric function $Y = Y(a_1, a_2, a_3, \ldots, a_n)$, it can be shown that (Smith, 1991):

$$\sigma_Y^2 \cong \sum_{v=1}^{n} \frac{\partial Y}{\partial a_v} \sum_{\lambda=1}^{n} \frac{\partial Y}{\partial a_\lambda} \left\langle (a_v - a_{0,v})(a_\lambda - a_{0,\lambda}) \right\rangle \quad (11)$$

The partial derivatives in Eq. (10) are calculated at $a = a_0$, where a_0 is the expectancy value of a. The parameter $\langle (a_v - a_{0,v})(a_\lambda - a_{0,\lambda}) \rangle$ is called *covariance* of a_v with respect to a_λ or $cov(a_v, a_\lambda)$ and usually has a non zero value. This value can be calculated from the partial uncertainties and the correlation factors $\rho_{v\lambda}$ involved:

$$cov(a_v, a_\lambda) = \sum_{k=1}^{m} \rho_{v,\lambda,k} \sigma_{v,k} \sigma_{\lambda,k} \quad (12)$$

where $k = 1, \ldots, m$ is the partial uncertainty index.

In the case where Y_i and Y_j represent k_0 or Q_0 factors from different targets, i and j, there will be additional correlations involving each pair of parameters, and the covariance between Y factors can be calculated as follows:

$$cov(Y_i, Y_j) \cong \sum_{v=1}^{n} \frac{\partial Y_i}{\partial a_v} \sum_{\lambda=1}^{n} \frac{\partial Y_j}{\partial a_\lambda} \left\langle (a_v - a_{0,v})_i \ (a_\lambda - a_{0,\lambda})_j \right\rangle \quad (13)$$

or

$$cov(Y_i, Y_j) \cong \sum_{v=1}^{n} \frac{\partial Y_i}{\partial a_v} \sum_{\lambda=1}^{n} \frac{\partial Y_j}{\partial a_\lambda} cov(a_{v,i}, a_{\lambda,j}) \quad (14)$$

The application of this methodology to Eq. (1) has been described in a previous paper by Dias et al. (2010). Eq. (2) corresponds to the intercept of Eq. (1), therefore the uncertainty in f comes directly from the fitting.

The derivatives involved in Q_0 determination are presented in the Appendix (Table A1). These formulae apply to Eq. (3)) coupled with Eq. (4), to be applied in Eqs. (11), (13) and (14).

The derivatives involved in k_0 determination are also presented in the Appendix (Table A2). These formulae apply to Eq. (5), to be applied in Eqs. (11), (13) and (14).

All partial errors involved in $A_{sp,i}$ and $A_{sp,c}$ determination were taken into account. However, the contribution of internal correlations between these partial errors to the overall uncertainties in k_0 and Q_0 was considered to be negligible in the present experiment.

3. Results and discussion

The behavior of the experimental peak efficiency as a function of the gamma-ray energy for the HPGe spectrometer is presented in Fig. 1. The efficiency results indicated by white marks correspond to Collodion standards. In this case, the covered gamma-ray energy range was between 244 and 1408 keV. The black marks correspond to IAEA standards. In this case, the covered gamma-ray energy range was between 53 and 1408 keV. In can be noted a maximum value around 80 keV.

Fig. 2 shows the behavior of percent residues for the two efficiency models described in Section 2.3, as a function of the gamma-ray energy. The error bars in the figure correspond to uncertainties in the experimental results. A good agreement can be observed between the experimental data and fitted values and corresponds to a 3rd degree polynomial in log–log scale, covering 244–1408 keV gamma-ray energy range. In this case, the reduced chi-square resulted 1.48. The second function is shown as black marks and corresponds to Eq. (10) covering 53–1408 keV gamma-ray energy range. In this case, the reduced chi-square resulted 0.80. The error bars are the percent uncertainty in the experimental efficiencies (one standard deviation). The sample activities determined by means of the two HPGe gamma-ray peak efficiency curves agreed within the uncertainty, estimated to be in the range of 0.5–0.9% for the energy interval of interest (328–1332 keV).

The results for f and α values are specific for the selected irradiation position near the IEA-R1 reactor core and resulted 49.7(19) and $-1.1(31)\times10^{-3}$, respectively. The latter value indicates an epithermal neutron field approaching the ideal spectrum in which α is equal to zero. As a result $Q_0(\alpha)$ approaches to value Q_0 according to Eq. (4).

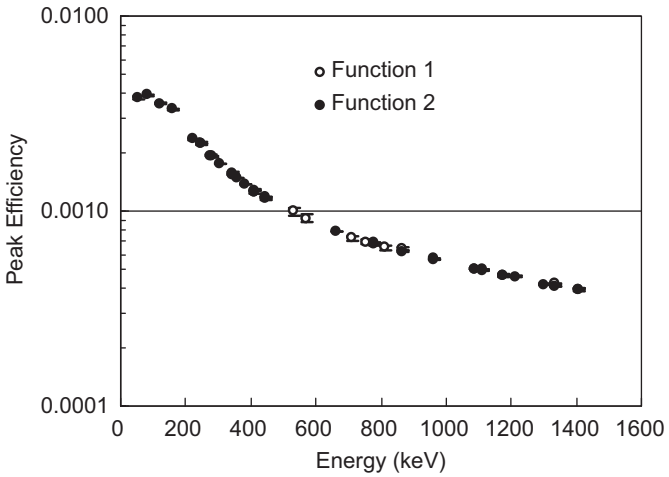

Fig. 1. Experimental peak efficiency, as a function of the gamma-ray energy. The white marks correspond to Collodion standards and the black marks to IAEA standards. The energy intervals were 244–1408 and 53–1408 keV, respectively.

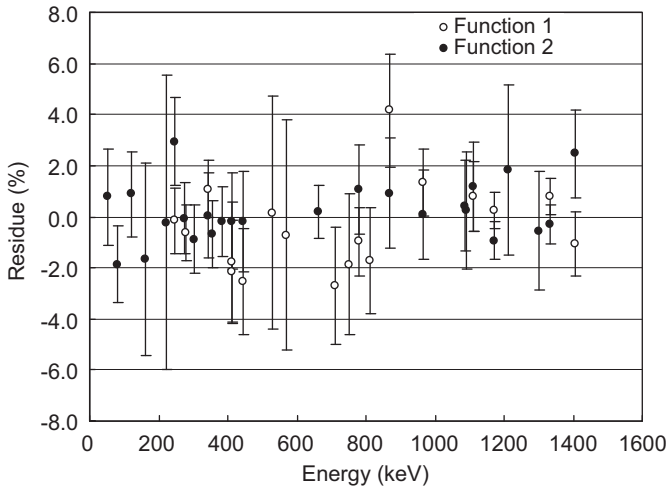

Fig. 2. Percent residues for the two fitting functions, applied to Collodion and IAEA standards, respectively. The white marks correspond to a 3rd degree polynomial in the log–log scale and the black marks correspond to Eq. (10). The energy intervals were 244–1408 and 53–1408 keV, respectively.

Table 3
Results obtained for k_0 and Q_0.

Reaction	Parameter	Present Work	Literature
$^{64}Zn(n,\gamma)^{65}Zn$	k_0	$5.63(8)\times10^{-3}$	$6.55(22)\times10^{-3}$ [a] $5.72(2)\times10^{-3}$ [b] $6.16(22)\times10^{-3}$ [c] $6.08(16)\times10^{-3}$ [d]
	Q_0	1.69(6)	1.908(94) [b] 1.73(9) [c]
$^{68}Zn(n,\gamma)^{69m}Zn$	k_0	$4.00(6)\times10^{-4}$	$4.10(17)\times10^{-4}$ [a] $3.98(2)\times10^{-4}$ [b,d]
	Q_0	2.34(4)	3.19(4) [b] 3.3(3) [c]

[a] Firestone, 2008.
[b] De Corte and Simonits, 2003.
[c] Mughabghab, 2006.
[d] Firestone, 2011.

The k_0 and Q_0 results are presented in Table 3. The number inside parentheses corresponds to the uncertainty in the last digits (one standard deviation). For ^{64}Zn the k_0 value agrees with De Corte and Simonits (2003), which corresponds to an experimental result, but it is not in agreement with either $6.55(22)\times10^{-3}$ from Firestone (2008) or with $6.16(22)\times10^{-3}$ from Mughabghab (2006). Recently the value taken from Firestone (2008) was amended to $6.08(16)\times10^{-3}$ in the final IAEA CRP report (Firestone, 2011). This latter value is in agreement with Mughabghab (2006) but is not in agreement either with De Corte and Simonits (2003) or with the present experiment. It should be pointed out, however, that those values from Firestone and Mughabghab were not obtained directly from experiment and depend on the gamma-ray probability per decay of the ^{65}Zn transition. This may be the cause of discrepancy.

For ^{64}Zn the Q_0 value agrees marginally with reference De Corte and Simonits (2003) but it is in good agreement with Mughabghab (2006). The latter value was calculated from the tabulated thermal cross section and resonance integral values.

The k_0 value for ^{68}Zn agrees well with all references within the estimated uncertainties, but Q_0 is not in agreement either with De Corte and Simonits (2003) or with Mughabghab (2006), which are in agreement with each other. This discrepancy indicates that new measurements should be performed in order to verify the correct value.

Table 4
Total uncertainties obtained for k_0 and Q_0 together with the corresponding correlation matrix.

Reaction	Parameter	Uncertainty (%)	Correlation matrix (× 1000)			
$^{64}Zn(n,\gamma)^{65}Zn$	k_0	1.4	1000			
	Q_0	3.3	−214	1000		
$^{68}Zn(n,\gamma)^{69m}Zn$	k_0	1.6	558	−191	1000	
	Q_0	1.7	−283	706	−371	1000

Table 4 shows the total uncertainty in each parameter and the corresponding correlation matrix. This information may be required when using the present results for other applications. The correlation factor between the two k_0 values is positive. This can be explained considering that the comparator (Au) is the same and contribute with identical components to Eq. (5). For the same reason, and considering Eq. (3), the correlation factor between the two Q_0 values is also positive. The correlation between k_0 and Q_0 values are negative. In this case, the comparator component appears in the denominator for k_0 and in the numerator for Q_0. Therefore, the raise in this component tends to decrease k_0 and increase the Q_0 value.

4. Conclusions

The k_0 and Q_0 factors were measured for ^{64}Zn and ^{68}Zn targets near the IEA-R1 research reactor core at a location were parameter α is very close to zero, indicating an almost ideal epithermal neutron field. The k_0 values for both ^{64}Zn and ^{68}Zn targets agreed well with De Corte and Simonits (2003) but only the value for ^{68}Zn agrees with Firestone (2008, 2011) and Mughabghab (2006). The value of Q_0 factor for ^{64}Zn reaction agreed well with Mughabghab (2006) but only marginally with De Corte and Simonits (2003). For ^{68}Zn target the Q_0 value from the present experiment does not agree with any value from the literature, indicating that new measurements are required to confirm the present results.

The present work applied covariance analysis for both k_0 and Q_0 measurements. A rigorous treatment was used taking into account all partial errors involved and their mutual correlations.

Acknowledgment

The authors are indebted to the National Council for Scientific and Technological Development (CNPq), from Brazil, for partial support of the present research work.

Appendix

See Tables A1 and A2.

Table A1
Partial derivatives involved in Q_0 determination.

Variable	Parameter	Partial derivative
a_1	$F_{cd,c}$	$\frac{A_{sp,c}G_{e,c}G_{th,i}\left(\frac{Q_{0,c}-0.429}{E_r^{\alpha}}+\frac{0.429}{(2\alpha+1)0.55^{\alpha}}\right)}{(A_{sp,c})_{Cd}\left(\frac{A_{sp,i}F_{Cd,i}}{(A_{sp,i})_{Cd}}-1\right)G_{e,i}G_{th,c}}$
a_2	$A_{sp,c}$	$\frac{F_{Cd,c}G_{e,c}G_{th,i}\left(\frac{Q_{0,c}-0.429}{E_r^{\alpha}}+\frac{0.429}{(2\alpha+1)0.55^{\alpha}}\right)}{(A_{sp,c})_{Cd}\left(\frac{A_{sp,i}F_{Cd,i}}{(A_{sp,i})_{Cd}}-1\right)G_{e,i}G_{th,c}}$

Table A1 (*continued*)

Variable	Parameter	Partial derivative
a_3	$(A_{sp,c})_{Cd}$	$-\dfrac{A_{sp,c}F_{Cd,c}G_{e,c}G_{th,i}\left(\frac{Q_{0,c}-0.429}{E_r^{\alpha}}+\frac{0.429}{(2\alpha+1)0.55^{\alpha}}\right)}{(A_{sp,c})_{Cd}^2\left(\frac{A_{sp,i}F_{Cd,i}}{(A_{sp,i})_{Cd}}-1\right)G_{e,i}G_{th,c}}$
a_4	$F_{Cd,i}$	$-\dfrac{A_{sp,i}\left(\frac{A_{sp,c}F_{Cd,c}}{(A_{sp,c})_{Cd}}-1\right)G_{e,c}G_{th,i}\left(\frac{Q_{0,c}-0.429}{E_r^{\alpha}}+\frac{0.429}{(2\alpha+1)0.55^{\alpha}}\right)}{(A_{sp,i})_{Cd}\left(\frac{A_{sp,i}F_{Cd,i}}{(A_{sp,i})_{Cd}}-1\right)G_{e,i}G_{th,c}}$
a_5	$A_{sp,i}$	$-\dfrac{\left(\frac{A_{sp,c}F_{Cd,c}}{(A_{sp,c})_{Cd}}-1\right)F_{Cd,i}G_{e,c}G_{th,i}\left(\frac{Q_{0,c}-0.429}{E_r^{\alpha}}+\frac{0.429}{(2\alpha+1)0.55^{\alpha}}\right)}{(A_{sp,i})_{Cd}\left(\frac{A_{sp,i}F_{Cd,i}}{(A_{sp,i})_{Cd}}-1\right)^2G_{e,i}G_{th,c}}$
a_6	$(A_{sp,i})_{Cd}$	$\dfrac{A_{sp,i}\left(\frac{A_{sp,c}F_{Cd,c}}{(A_{sp,c})_{Cd}}-1\right)F_{Cd,i}G_{e,c}G_{th,i}\left(\frac{Q_{0,c}-0.429}{E_r^{\alpha}}+\frac{0.429}{(2\alpha+1)0.55^{\alpha}}\right)}{(A_{sp,i})_{Cd}^2\left(\frac{A_{sp,i}F_{Cd,i}}{(A_{sp,i})_{Cd}}-1\right)^2G_{e,i}G_{th,c}}$
a_7	$G_{th,i}$	$\dfrac{\left(\frac{A_{sp,c}F_{Cd,c}}{(A_{sp,c})_{Cd}}-1\right)G_{e,c}\left(\frac{Q_{0,c}-0.429}{E_r^{\alpha}}+\frac{0.429}{(2\alpha+1)0.55^{\alpha}}\right)}{\left(\frac{A_{sp,i}F_{Cd,i}}{(A_{sp,i})_{Cd}}-1\right)G_{e,i}G_{th,c}}$
a_8	$G_{e,c}$	$\dfrac{\left(\frac{A_{sp,c}F_{Cd,c}}{(A_{sp,c})_{Cd}}-1\right)G_{th,i}\left(\frac{Q_{0,c}-0.429}{E_r^{\alpha}}+\frac{0.429}{(2\alpha+1)0.55^{\alpha}}\right)}{\left(\frac{A_{sp,i}F_{Cd,i}}{(A_{sp,i})_{Cd}}-1\right)G_{e,i}G_{th,c}}$
a_9	$G_{th,c}$	$-\dfrac{\left(\frac{A_{sp,c}F_{Cd,c}}{(A_{sp,c})_{Cd}}-1\right)G_{e,c}G_{th,i}\left(\frac{Q_{0,c}-0.429}{E_r^{\alpha}}+\frac{0.429}{(2\alpha+1)0.55^{\alpha}}\right)}{\left(\frac{A_{sp,i}F_{Cd,i}}{(A_{sp,i})_{Cd}}-1\right)G_{e,i}G_{th,c}^2}$
a_{10}	$G_{e,i}$	$-\dfrac{\left(\frac{A_{sp,c}F_{Cd,c}}{(A_{sp,c})_{Cd}}-1\right)G_{e,c}G_{th,i}\left(\frac{Q_{0,c}-0.429}{Er^{\alpha}}+\frac{0.429}{(2\alpha+1)0.55^{\alpha}}\right)}{\left(\frac{A_{sp,i}F_{Cd,i}}{(A_{sp,i})_{Cd}}-1\right)G_{e,i}^2G_{th,c}}$
a_{11}	$Q_{0,c}$	$\dfrac{\left((A_{sp,c}F_{Cd,c}/(A_{sp,c})_{Cd})-1\right)G_{e,c}G_{th,i}}{Er^{\alpha}\left((A_{sp,i}F_{Cd,i}/(A_{sp,i})_{Cd})-1\right)G_{e,i}G_{th,c}}$
a_{12}	E_r	$-\dfrac{\alpha Er^{-(\alpha+1)}\left(\frac{A_{sp,c}F_{Cd,c}}{(A_{sp,c})_{Cd}}-1\right)G_{e,c}G_{th,i}(Q_{0,c}-0.429)}{\left(\frac{A_{sp,i}F_{Cd,i}}{(A_{sp,i})_{Cd}}-1\right)G_{e,i}G_{th,c}}$
a_{13}	α	$\left(\frac{A_{sp,c}F_{Cd,c}}{(A_{sp,c})_{Cd}}-1\right)G_{e,c}G_{th,i}\times\dfrac{\left(-\frac{\log(E_r)(Q_{0,c}-0.429)}{Er^{\alpha}}+\frac{0.2565}{(2\alpha+1)0.55^{\alpha}}-\frac{0.858}{(2\alpha+1)^20.55^{\alpha}}\right)}{\left(\frac{A_{sp,i}F_{Cd,i}}{(A_{sp,i})_{Cd}}-1\right)G_{e,i}G_{th,c}}$

Table A2
Derivatives involved in k_0 determination.

Variable	Parameter	Partial derivative
a_1	$A_{sp,i}$	$\dfrac{\varepsilon_cG_{th,c}}{\varepsilon_i\left(A_{sp,c}-\left((A_{sp,c})_{Cd}/F_{Cd,c}\right)\right)G_{th,i}}$
a_2	$(A_{sp,i})_{Cd}$	$-\dfrac{\varepsilon_cG_{th,c}}{\varepsilon_i\left(A_{sp,c}-\left((A_{sp,c})_{Cd}/F_{Cd,c}\right)\right)F_{Cd,i}G_{th,i}}$
a_3	$F_{Cd,i}$	$\dfrac{(A_{sp,i})_{Cd}\varepsilon_cG_{th,c}}{\varepsilon_i\left(A_{sp,c}-\left((A_{sp,c})_{Cd}/F_{Cd,c}\right)\right)(F_{Cd,i})^2G_{th,i}}$
a_4	$A_{sp,c}$	$-\dfrac{\varepsilon_c\left(A_{sp,i}-\left((A_{sp,i})_{Cd}/F_{Cd,i}\right)\right)G_{th,c}}{\varepsilon_i\left(A_{sp,c}-\left((A_{sp,c})_{Cd}/F_{Cd,c}\right)\right)^2G_{th,i}}$
a_5	$(A_{sp,c})_{Cd}$	$\dfrac{\varepsilon_c\left(A_{sp,i}-\left((A_{sp,i})_{Cd}/F_{Cd,i}\right)\right)G_{th,c}}{\varepsilon_i\left(A_{sp,c}-\left((A_{sp,c})_{Cd}/F_{Cd,c}\right)\right)^2F_{Cd,c}G_{th,i}}$
a_6	$F_{Cd,c}$	$-\dfrac{(A_{sp,c})_{Cd}\varepsilon_c\left(A_{sp,i}-\left((A_{sp,i})_{Cd}/F_{Cd,i}\right)\right)G_{th,c}}{\varepsilon_i\left(A_{sp,c}-\left((A_{sp,c})_{Cd}/F_{Cd,c}\right)\right)^2(F_{Cd,c})^2G_{th,i}}$

Table A2 (*continued*)

Variable	Parameter	Partial derivative
a_7	$G_{th,c}$	$\dfrac{\varepsilon_c\left(A_{sp,i}-\left((A_{sp,i})_{Cd}/F_{Cd,i}\right)\right)}{\varepsilon_i\left(A_{sp,c}-\left((A_{sp,c})_{Cd}/F_{Cd,c}\right)\right)G_{th,i}}$
a_8	$G_{th,i}$	$-\dfrac{\varepsilon_c\left(A_{sp,i}-\left((A_{sp,i})_{Cd}/F_{Cd,i}\right)\right)G_{th,c}}{\varepsilon_i\left(A_{sp,c}-\left((A_{sp,c})_{Cd}/F_{Cd,c}\right)\right)(G_{th,i})^2}$
a_9	ε_c	$\dfrac{\left(A_{sp,i}-\left((A_{sp,i})_{Cd}/F_{Cd,i}\right)\right)G_{th,c}}{\varepsilon_i\left(A_{sp,c}-\left((A_{sp,c})_{Cd}/F_{Cd,c}\right)\right)G_{th,i}}$
a_{10}	ε_i	$-\dfrac{\varepsilon_c\left(A_{sp,i}-\left((A_{sp,i})_{Cd}/F_{Cd,i}\right)\right)G_{th,c}}{(\varepsilon_i)^2\left(A_{sp,c}-\left((A_{sp,c})_{Cd}/F_{Cd,c}\right)\right)G_{th,i}}$

References

De Corte, F., Simonits, A., 2003. Recommended nuclear data for use in the k_0 standardization of neutron activation analysis. At. Data Nucl. Data Tables 85, 47–67.

De Corte, F., 1987. The k_0 Standardization Method—A Move to the Optimization of Neutron Activation Analysis, Rijksuniversiteit Gent.

Dias, M.S., Cardoso, V., Koskinas, M.F., Yamazaki, I.M., 2010. Determination of the neutron spectrum shape parameter α in k_0 NAA methodology using covariance analysis. Appl. Radiat. Isot. 68, 592.

Dias, M.S., Cardoso, V., Vanin, V.R., Koskinas, M.F., 2004. Combination of nonlinear function and mixing method for fitting HPGe efficiency curve in the 59–2754 keV energy range. Appl. Radiat. Isot. 60 (5), 683.

ENDF/B-VII.0 Cross Section Library, 2010. URL ⟨http://www.nndc.bnl.gov⟩.

Firestone, R.B., 2008. Comparison of neutron activation analysis k_0 and σ_0 data. Lawrence Berkeley National Laboratory, Berkeley CA. In: Proceedings of the Third Co-ordination Meeting on a Reference Database for Neutron Activation Analysis, 17–19 November 2008—IAEA, Vienna.

Firestone, R.B., 2011. Private communication.

Kodeli, I., Trkov, A., 2007. Validation of the IRDF-2002 dosimetry library. Nucl. Instrum. Methods Phys. Res. A 577, 664–681.

Kolotov, V.P., De Corte, F., 2002. Compilation of k_0 and Related Data for NAA in the Form of Electronic Database. International Union of Pure and Applied Chemistry (IUPAC).

Martinho, E., Salgado, J., Gonçalves, I.F., 2004. Universal curve of thermal neutron self-shielding factor in foils, wires, spheres and cylinders. J. Radioanal. Nucl. Chem. 261 (3), 637.

Martinho, E., Salgado, J., Gonçalves, I.F., 2003. Universal curve of epithermal neutron self-shielding factor in foils, wires and spheres. Appl. Radiat. Isot. 58, 371.

Mughabghab, S.F., 2006. Atlas of Neutron Resonances. Elsevier, Amsterdam.

Smith, D.L., 1991. Probability, statistics, and data uncertainties in Nuclear Science and Technology. Series: Neutron Physics and Nuclear Data in Science and Technology. Published by American Nuclear Society.

Zevallos-Chávez, J.Y., Genezini, F.A., Zamboni, C.B., Cruz, M.T.F., Martins, M.N., Vanin, V.R., 2005. Analysis of $\gamma-\gamma$ directional correlation data taken with a multi-detector system. Rev. Sci. Instrum. 76, 1.